Journal of Engg. Research **Vol. 2 No. (4) Dec 2014** pp. 67-86

إعادة بناء كفاءة محول Curvelet للتصوير بالرنين المغناطيسي

***رشيد حسين **وعبد الرحمن ميمون**

* أستاذ مشارك ونائب مدير كلية الدراسات العليا في العلوم الهندسية وتكنولوجيا المعلومات، كلية العلوم والهندسة والتكنولوجيا، جامعة هامدارد. كراتشي، باكستان.

** أستاذ في كلية العلوم والهندسة والتكنولوجيا، جامعة هامدارد. كراتشي، باكستان.

الخلاصـة

ترتبط كفاءة التحويلات بعمق مع معالجة الصور، والحوسبة العلمية والرؤية للكمبيوتر. يركز هذا البحث على أداء محول Curvelet للصور بالرنين المغناطيسي. وتتضمن النتيجة الرئيسية لهذه التقنية إزالة الضوضاء الغير متجانسة باستخدام أساليب Curvelet. وينتمي Curvelet إلى عائلة من مويجات الموجهة. ومحول Curvelet ليس فقط يحتوي على ترجمات والتوسعات ولكن أيضا التناوب والتي يمكن أن تحسن إعادة بناء الأجسام المنحنية. يتضمن هذا البحث إعادة بناء المتعددة للأجسام مع حافة الانقطاع. تظهر النتائج التجريبية بأن المحول Curvelet لديه القدرة فائقة على إعادة ابناء الصورة مع الأجسام المنحنية. والطور أخرى لهذا البحث يغطي تقسيم الصور الضجيجية باستخدام FCM الخوارزمية. ويستند تشكيل العنقودية في خوارزمية FCM على المسافة الإقليدية بين بكسل مع كثافة المماثلة. وتظهر النتائج التجريبية بأن إعادة بناء تقسيم الصور تتأثر سلبا من رشقات الضوضاء .

Reconstruction performances of curvelet transform for magnetic resonance images

RASHID HUSSAIN* AND ABDUL REHMAN MEMON**

** Associate Professor and Chairman, Deparment of Electrical Engineering, Faculty of Engineering Science and Technology, Hamdard University Karachi 74600, Pakistan. rashid.hussain@hamdard.edu.pk*

*** Professor, Faculty of Engineering Science and Technology , Hamdard University, Karachi 74600, Pakistan.*

ABSTRACT

Reconstruction performances of transforms are deeply associated with image processing, scientific computing and computer vision. This research focuses on the performance of Curvelet Transform for Magnetic Resonance Images. The main outcome of this technique includes the removal of non-homogeneous noise using Curvelet based de-noising methods. Curvelet Transform belongs to the family of directional Wavelets. Curvelet Transform not only contains translations, dilations but also the rotations, which can enhance the reconstruction of curve objects. This research involves multi-scale reconstruction of objects with edge discontinuities. Experimental results show that Curvelet Transform has superior reconstruction capability for an image with curve objects. Another phase of this research covers the segmentation of de-noised images using Fuzzy C-Means Clustering (FCM) algorithm. The cluster formation in FCM algorithm is based on the Euclidian distance between pixels with similar intensities. Experimental results show that segmentation of reconstructed images is adversely affected by the noise bursts.

Keywords: Clustering; curvelet transform; de-noised image; image segmentation; wavelet transform.

INTRODUCTION

Wavelets have limitations when reconstructing the smoothness across edges and contour in the images, they are more suitable for reconstructing the sharp points across lines or edges. Several studies have been conducted to overcome these limitations using directional Wavelets such as Curvelet and Ridgelet Transforms (Feng *et al*., 2007; Chen G.Y. & Kégl B. 2007; Bo Zheng *et al*., 2008; Candès & D.L. Donoho, 1998; Starck *et al*., 2002).

Rigdelet Transform is effective for radial direction. Unfortunately, medical images comprise of curves and therefore rigdelet is not suitable for image segmentation. Edges, curves and contours are one of the difficult objects to reconstruct with conventional Wavelet. Donoho and Starck are considered as the pioneers in Curvelet and Ridglet Transforms. In the second generation Curvelet Transform, Ridgelet Transform is no longer use in the pre-processing steps, which results in reduce computational complexity (Candès & D.L. Donoho, 1999; Starck *et al*., 2002). Another extension of Direction Wavelet is Contourlets. It is developed by Do and Vetterli in 2005. Contourlets have the ability to reconstruct contours and edges at various orientations. This transform is developed for multi-scale representation of objects with edge discontinuities (Do & Vetterli, 2005).

Curvelet not only contains translations, dilations (as in case of Wavelet) but also the rotations. Curvelet Transform involves the decomposition of the image into respective subbands. Later each subband is spatially partitioned and finally the Ridgelet Transform is applied to spatially partitioned subbands (Candès & D.L. Donoho, 1999).

Ridgelet Transform was proposed by Candes in 1998 and further developed by Donoho and Starck in 2002 (Starck *et al*., 2002).

For 2D function *f*, we work throughout in two dimensions with spatial variable $x \in R2$, for each scale $a > 0$, $\theta \in [0, 2\pi)$ is angular variable, b is the position of the Ridgelet Transform R_f:

$$R_f(a,b,\theta) = \int \psi_{a,b,\theta}(x) f(x) dx \tag{1}$$

Ridgelet function $\psi_{a,b,\theta}(x)$ in (1) is defined as:

$$\psi_{a,b,\theta}(x) = a^{\frac{1}{2}} \psi\left(\frac{x_1 \cos(\theta) + x_2 \sin(\theta) - b}{a} \right) \tag{2}$$

It is shown from above (1) and (2), that the Ridgelet Transform demonstrate directional property. This function is constant along lines $x_1 \cos\theta + x_2 \sin\theta$. The continues Ridgelet coefficients of an object *f* are given by the analysis of the Radon Transform RA_f. It converts singularities along lines into point singularities (Starck *et al*., 2002).

$$R_f(a,b,\theta) = \int RA_f(\theta,t) \psi\left(\frac{t-b}{a}\right) dt \tag{3}$$

There are major limitations with Ridgelet Transform in terms of discontinuities along the edges of the image. These discontinuities will result in a large number of non-zero coefficients and increasing computational complexity.

Some of the recent research in this domain includes; Bionic vision-based synthetic aperture radar image edge detection method in non-sub sampled Contourlet Transform domain Radar, Sonar and Navigation. In this research, edge extractions were performed on real and simulated SAR images, which showed that proposed methods is better than other edge extraction methods (Li, Q. *et al*., 2012). Retinal image analysis using Curvelet Transform and multistructure elements morphology by reconstruction. In this research a simple thresholding method applied for blood vessel detections (Miri M. *et al.,* 2011). Water reflection recognition based on motion blur invariant moments in Curvelet Space. In the proposed method effective classification of water reflection images were performed using novel water reflection recognition technique (Sheng H. *et al.,* 2013). Image quality assessment based on multiscale geometric analysis. In the proposed framework multiscale geometric analysis offers various transforms including Curvelet, Bandelet, and Contourlet transforms to capture image geometrical information (Xinbo G. *et al.,* 2009). Hybrid no-reference natural image quality assessment of noisy, blurry JPEG2000 and JPEG images. In this paper, image quality assessment was based on hybrid of Curvelet, Wavelet, and Cosine Transforms (Shen Ji & Qin Li, 2011). An accurate multimodal 3-D vessel segmentation method based on brightness variations on OCT layers and Curvelet domain fundus image analysis. In this proposed method the authors exploit the fact that retinal nerve fiber becomes thicker in the presence of blood (Kafieh, R. *et al.,* 2013). Automatic detection of exudates and optic disk in retinal images using Curvelet Transform. In this technique automatic detection of optical disk is applied for potential clinical parameters for diagnosis of retinopathic diseases (Esmaeili, M. *et al.,* 2012). Several other studies have been conducted to de-noise images using directional Wavelet (Feng *et al*., 2007; G.Y.Chen *et al*., 2007; Bo Zheng *et al*., 2008; Candès & D.L. Donoho, 1999; Starck *et al*., 2002).

Comparison of Curvelet, Ridgelet and Wavelet Transforms is shown in Table 1, while the properties of first and second generation of Curvelet Transforms are shown in Table 2.

In this research, we have investigated the removal of non-homogeneous noise using Curvelet Transform. In this analysis, we also demonstrated the effects of noise patterns on the computational performance of Fuzzy C-Means Clustering (FCM) algorithm.

Table 1: Comparison of Curvelet , Ridgelet and Wavelet Transforms

Properties	Curvelet	Ridgelet	Wavelet
Segmentation of malignant areas	Efficiently segmented abnormal tissues in noisy image	Not efficient as it only support linear radial structure	In this study segmentation is complement using (FCM) algorithm.
Directionality and anisotropy	High degree of directionality and Anisotropy	High degree of directionality across the ridges of image	Low degree of directionality and Anisotropy
Singularity approx.	Few coefficients required	Suitable for Line singularities, which is good for edge detection	Suitable for only point singularities
Localization	Yes	Yes	Yes
Multi resolution analysis	Yes	Yes	In this study multi resolution analysis is used to identify noise burst
Complexity	Simple, faster and Less Redundant	High	High
De-noising capabilities	High	Low	Low

Table 2: Generations of Curvelet Transform.

Properties	First Generation	Second Generation
Edges representation	Ridgelet are not efficiently represents curve edges.	Not efficient, as it only support linear radial structure
Computational complexity	High computational complexity for large scale data.	It has low computational complexity due to its simpler structure. Second generation does not use Rigdelet.
Redundancy level	Redundancy level is high in First generation due to the overlapping window used for avoiding blocking effects.	Redundancy level is high in Second generation due to the tight frame expansion
Constructed based	Discrete Ridgelet Transform	Bandpass Filtering in Fourier Domain
Multi resolution analysis	Yes	Yes

METHODOLOGY

A. Image synthesis with homogenous and non-homogenous noise

Two phases of image synthesis involves homogenous and non-homogenous noise. In the first set of synthesis Adaptive White Gaussian Noise (AWGN) is uniformly distributed across the entire image as shown in Figure 1. In the second set of synthesis, Adaptive White Gaussian Noise (AWGN) distributed non-homogenously across the image as shown in Figure 5.

B. Noise estimation using robust median estimator

Once the image synthesis is performed, the next step is noise estimation through variance σ^2. The robust median estimator projected noise variance from the sub-band region *HH1* of Wavelet Transform (Gonzalez & Wood, 2002) as shown in (4).

$$\sigma = \frac{Median\left(\left|cwd(x,y)\right|\right)}{0.6745} \tag{4}$$

where *cwd(x,y)* are the Wavelet diagonal detail coefficients.

C. Applying soft thresholding technique for de-noising

In this research phase, thresholds are individually applied at each resolution of the image using Stein Unbiased Risk Estimator (SURE) shrink thresholding. SureShrink is an adaptable soft thresholding technique. The overall computational complexity of this approach is of the order of *Nlog(N),* where *N* is the sample size. This method is adaptive with discontinuities on the smooth background (Donoho D., 1995).

D. Performance assessment of reconstructed images

Image quality matrix Peak Signal to Noise Ratio (PSNR) has been used for accessing the performance of original, noisy and de-noised image. *R* returns the PSNR, it is the measure of peak error in the pixel values of two sets of images, as shown in (5),

$$R = 10\log_{10}\left(\frac{gray\ \max^2 * numel(x)}{norm(x - xr, fro)^2}\right) \tag{5}$$

Where x and xr represents the pixel values of original and reconstructed images respectively. Graymax is the maximum grey value possible; the default value is 255, *numel* is the number of elements in an array *Fro* is the Frobenius norm.

E. Image segmentation using fuzzy clustering algorithm

This research phase aims at segmenting objects of interest in Curvelet Transform based reconstructed images. For this purpose famous Fuzzy C-Means Clustering algorithm (Hussain *et al*., 2002; Wen L., *et.al,* 2006; Lyer NS., *et.al,* 2002; Bezdek J., *et.al,* 1981; Cannon R., *et.al,* 1986; Dunn J., *et.al,* 1973) applied on various sets of images. The computational complexity of Fuzzy C-Means Clustering algorithm expound for clean, noisy and de-noised images.

RESULTS AND DISCUSSION

De-noising using curvelet transform

This implementation has been performed using Matlab based implementation of Curvelet and Ridgelet. In this research, the test images went under different sets of analysis. In Figure 1, the visual results of a set of noisy knee images (Knee-5) are presented.

Along the first row, figure 1(a) represents Knee-5 a noisy image (Noise level = 10dB); this noise level results in poor visibility of the image. The noise is distributed homogeneously over the entire image. Figure 1(b) represents Knee-5 a de-noised image using Curvelet Transform; the results showed that the image is visually better than that of Wavelet de-noised image. Figure 1(c) represents an original image in gif format. Converting other formats into gif will introduce additional noise. Along the

second row, figure 1(d) corresponds to Knee-5 noisy image (Noise level = 20dB), the noise level get doubled and have impact on de-noising process. Figure 1(e) corresponds to Knee-5 de-noised image using Curvelet Transform, this process results in better reconstructed image. Figure 1(f) corresponds to original image. The image conversion should be accounted for further research, as it contributes to additional image deformation. Along the third row, figure 1(g) describes Knee-5 a noisy image (Noise level= 30dB); the increasing noise level results in poor image reconstruction. Figure 1(h) describes Knee-5 a de-noised image using Curvelet Transform. Figure 1(i) represents original image in gif format. Along the fourth row, figure 1(j) describes Knee-5 a noisy image (Noise level= 40dB); the increasing noise level results in poor image reconstruction. Figure 1(k) describes Knee-5 a de-noised image using Curvelet Transform. Figure 1(l) represents an original image in gif format. Results showed that the Curvelet based de-noising is better than Wavelet based de-noising. Results showed that *png* format cannot use directly.

In Figure 2 the visual results of a set of noisy brain images (Brain-18) are presented.

Along the first row, figure 2(a) illustrates Brain-18 a noisy image (Noise level= 10dB), lower values yields poor visibility of the image. Figure 2(b) illustrates Brain-18 a de-noised image using Curvelet Transform; it has been observed that the image is smoother across the edges of the image. Figure 2(c) illustrates an original image of the brain with no additional deformities. Along the second row, figure 2(d) exemplifies Brain-18 a noisy image (Noise level= 20dB), with higher noise level compared to the last image. Figure 2(e) exemplifies Brain-18 a de-noised image using Curvelet Transform, the de-noised image is far better than its original counterpart figure 2(f). It is selected carefully to meet the requirements of the image reconstruction using Curvelet Transform. Along the third row, figure 2(g) demonstrates Brain-18 a noisy image (Noise level= 30dB); higher noise level results in visually better de-noised images. Figure 2(h) demonstrates Brain-18 a de-noised image, using Curvelet Transform. Figure 2(i) demonstrates an original image with the same format (gif). Along the fourth row, figure 2(j) describes Brain-18 a noisy image (Noise level= 40dB), the increasing noise level results in poor image reconstruction. Figure 2(k) describes Brain-18 a de-noised image using Curvelet Transform. Figure 2(l) represents an original image in gif format. Results showed that the Curvelet based de-noising is better than Wavelet based de-noising. Both Figure 1 and Figure 2 shows consistent performance in terms of image reconstruction, which further validate research findings.

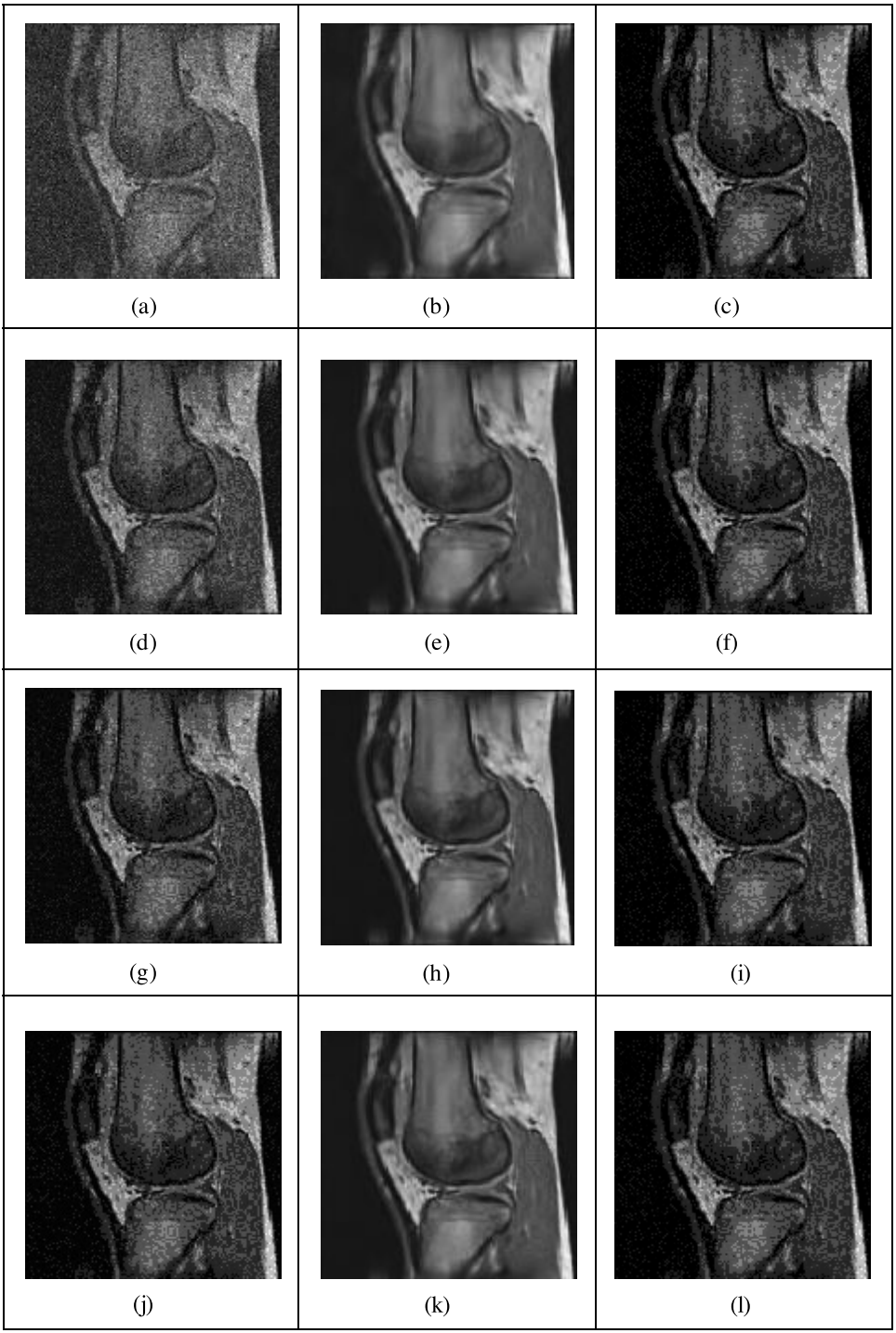

Fig. 1. Visual results of different set of de-noised (homogenous) knee-5 images using Curvelet Transform.

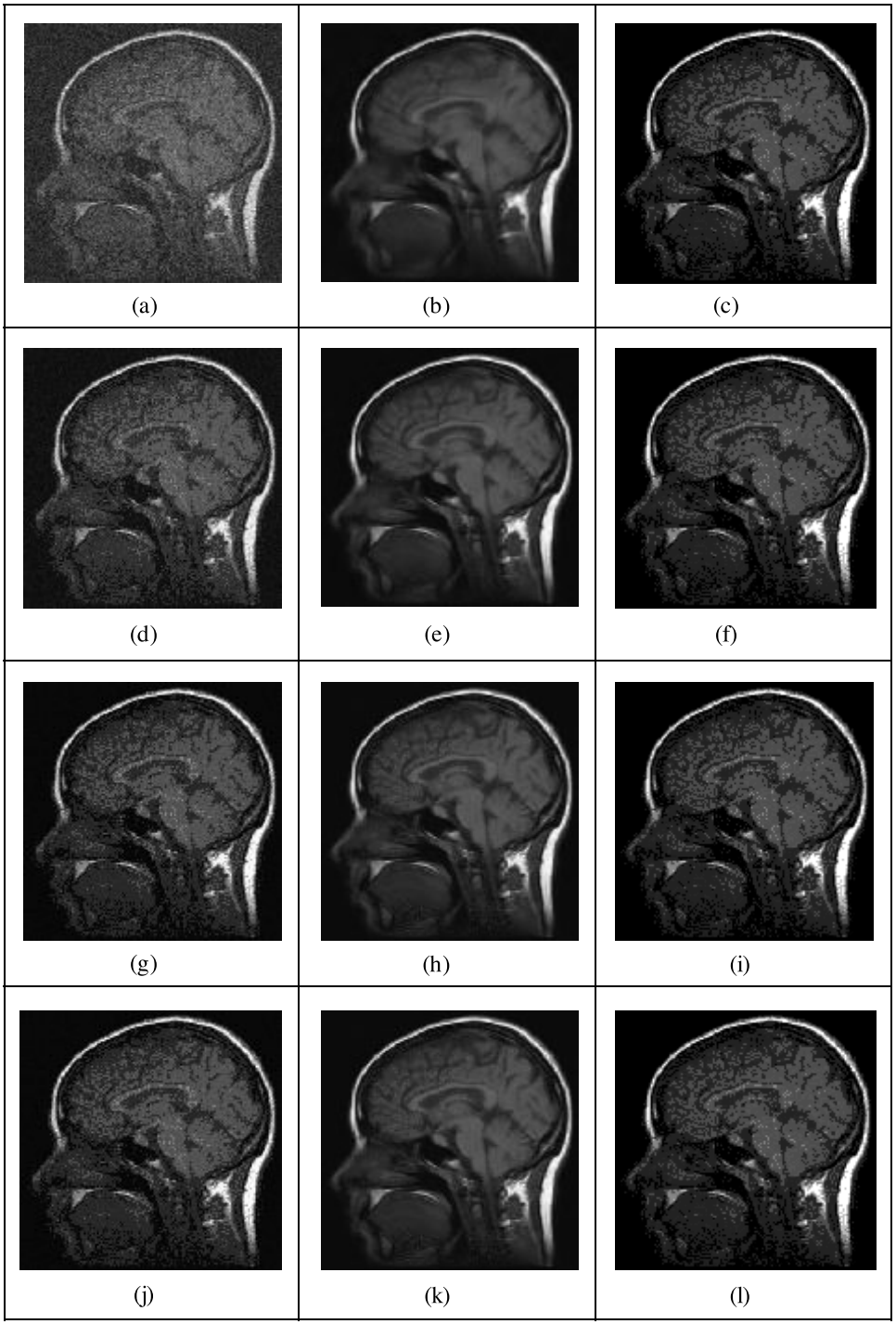

Fig. 2. Visual results of different set of de-noised (homogenous) Brain-18 images using Curvelet Transform.

Quality assessment of curvelet transform based de-noised images

The image quality assessment using Mean Square Error (MSE) with various noise levels Adaptive White Gaussian Noise (AWGN) is shown in Table 3 and Figure 3. Similarly Peak Signal to Noise Ratio for quality assessment is shown in Table 4 and Figure 4.

MSE1 is the assessment between original and noisy image,

MSE2 is the assessment between Curvelet Transform based de-noised and noisy images,

MSE3 is the assessment between original and Curvelet Transform based de-noised images.

At a lower value of noise level (10 (dB)), MSE1 is at a higher level (2977) and for higher value of noise level ($\sigma = 0.040$ (dB)), MSE1 is at a lower level (470.0652). This assessment shows that lower noise levels yield more error between a clean and noisy image. A similar assessment has been performed for MSE2and MSE3. Smaller values of MSE's show the effectiveness of the Curvelet based de-noising.

PSNR1 is the estimation between original and noisy image,

PSNR2 is the estimation between de-noised and noisy images,

PSNR3 is the estimation between original and de-noised images.

At a lower value of noise level (10 (dB)), PSNR1 is at a lower level (13.4264) and for higher values of noise level ($\sigma = 0.040$ (dB)), PSNR1 is at a higher level (21.4432). This estimation shows that the lower noise levels results in more error between a clean and noisy image. A similar estimation has been performed for PSNR2 and PSNR3. Smaller values of PSNR's show the effectiveness of the Curvelet Transform based reconstruction.

Table 3. Mean Square Error (MSE) estimations for different values of standard deviations (Brain-3) using Curvelet tranform

AWGN	MSE-1	MSE-2	MSE-3
WN = 10	2.9774e+003	1.6897e+003	1.0449e+003
WN = 20	1.0719e+003	1.0110e+003	1.0865e+003
WN = 30	611.8802	776.8353	729.0705
WN = 40	470.0652	723.8664	722.5475

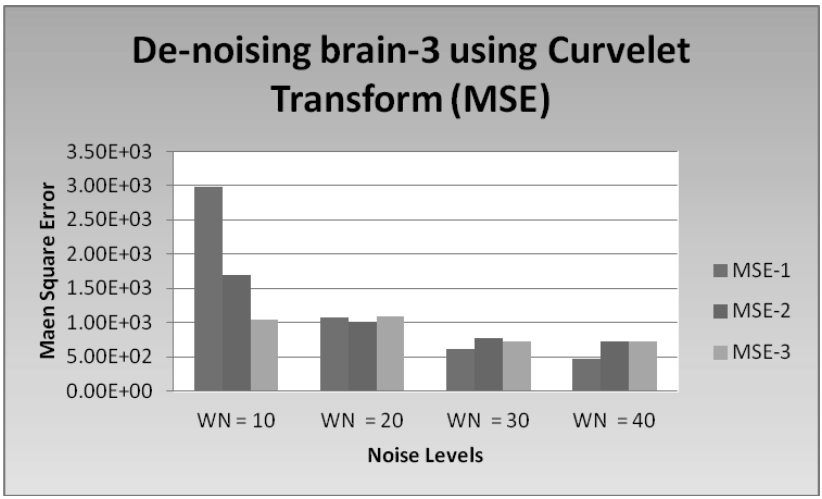

Fig. 3. Mean Square Error (MSE) estimations for different values of standard deviations (Brain-3) using Curvelet Transform.

Table 4. Peak Signal to Noise Ratio (PSNR) estimations for different values of standard deviations (Brain-3) using Curvelet Transform.

AWGN	PSNR -1	PSNR -2	PSNR -3
WN = 10	13.4264	15.8868	17.9740
WN = 20	17.8635	18.1174	17.8046
WN = 30	20.2981	19.2615	19.5371
WN = 40	21.4432	19.5682	19.5761

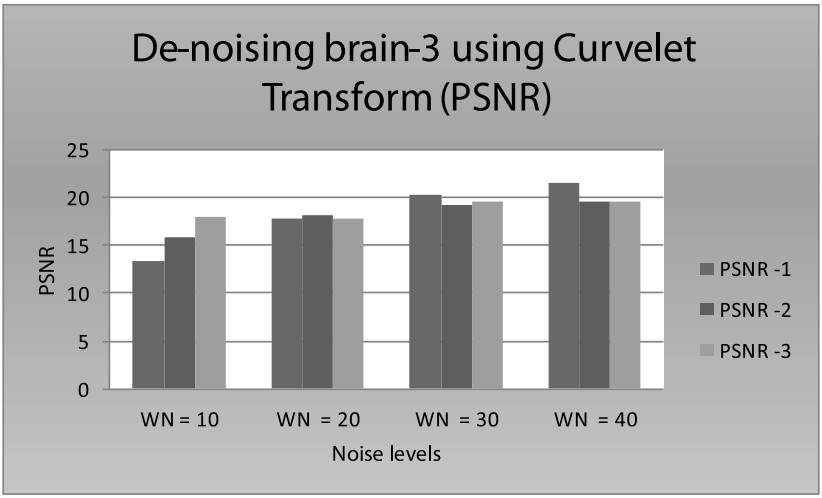

Fig. 4. Peak Signal to Noise Ratio (PSNR) estimations for different values of standard deviations (Brain-3) using Curvelet Transform.

Non-homogeneous de-noising using curvelet transform

The test images went under a different set of analysis. In Figure 5, the visual results of non-homogeneous noisy brain images (Brain-2 to Brain-5) are presented.

Along the first row, figure 5(a) shows Brain-2 as a non-homogeneous noisy image; a noise burst of considerable size has been added and it is not noticeable. Figure 5(b) shows Brain-2 a de-noised image using Curvelet Transform; the effectiveness of de-noised method has been investigated for non-homogeneous noise bursts. Figure 5(c) show an original image has no malignant areas; therefore it will not provide any pattern of interest. Along the second row, figure 5(d) exhibits Brain-3 a noisy image; it has noise burst over the malignant pattern. Figure 5(e) exhibits Brain-3 a de-noised image using Curvelet Transform; results showed that Curvelet demonstrate better results for de-noising. Figure 5(f) exhibits an original image with a prominent tumor. Along the third row, figure 5(g) represents Brain-4 a noisy image; the size of the noise burst is similar compared to the last image sample. Figure 5(h) represents Brain-4 a de-noised image using Curvelet Transform. Figure 5(i) represents an original image with medium size tumor. Along the fourth row, figure 5(j) signifies Brain-5 a noisy image; the noise is confined at a small portion of the image, and here in this case the noise burst is covering the entire malignant pattern. Figure 5(k) signifies Brain-5 a de-noised image using Curvelet Transform and this de-noised image is very important for detecting malignant patterns in non-homogeneous noisy image. Further investigations are required to improve the reconstruction of a noisy image with small object of interest. Figure 5(l) signifies an original image with small pattern of interest. Along the fifth row, figure 5(m) demonstrates Brain-6 a noisy image, with no tumor or malignant areas. Figure 5(n) demonstrates Brain-6 a de-noised image using Curvelet Transform, it will be further used to investigate the false detection of malignant patterns using image segmentation. Figure 5(o) demonstrates an original image. It is observed that noise burst will increase the false alarm.

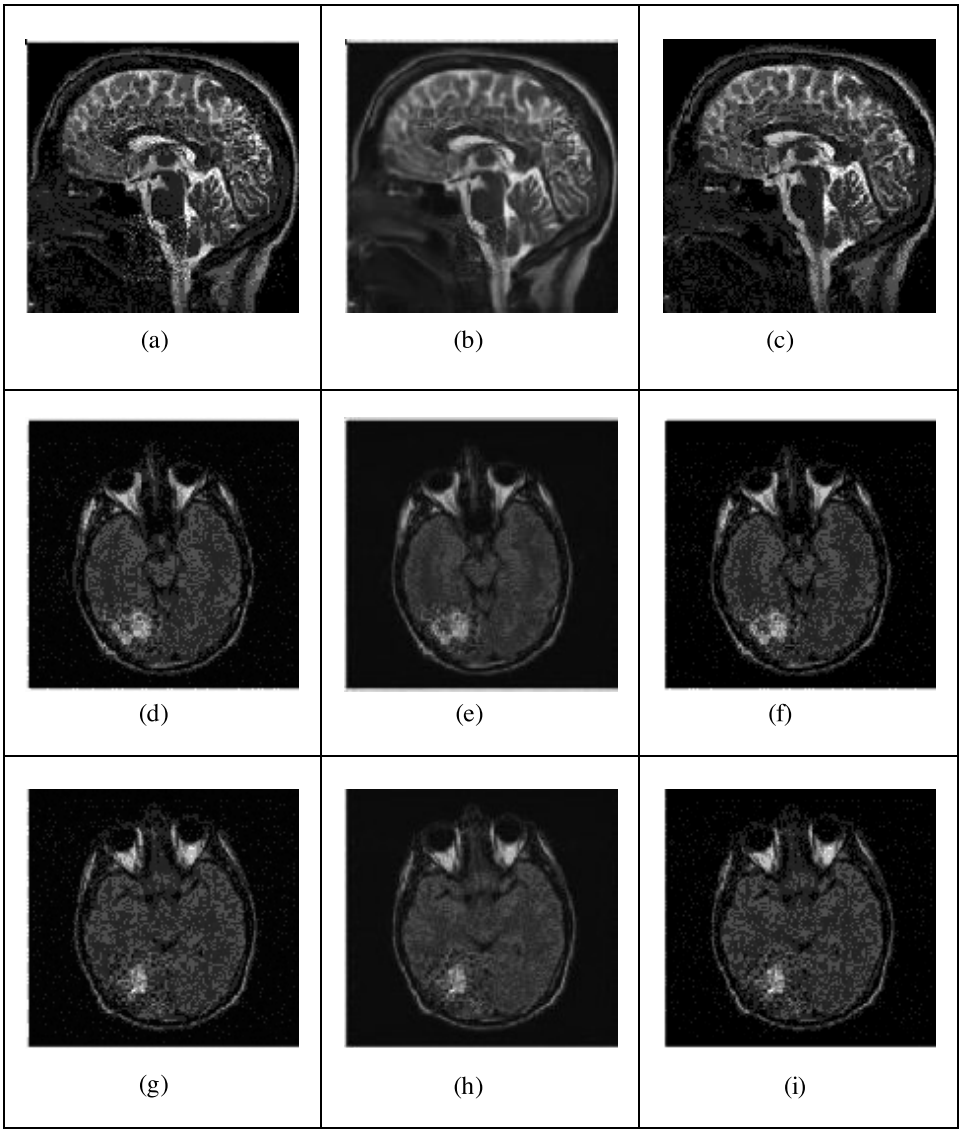

Fig. 5. Visual results of different set of de-noised brain images using Curvelet Transform.

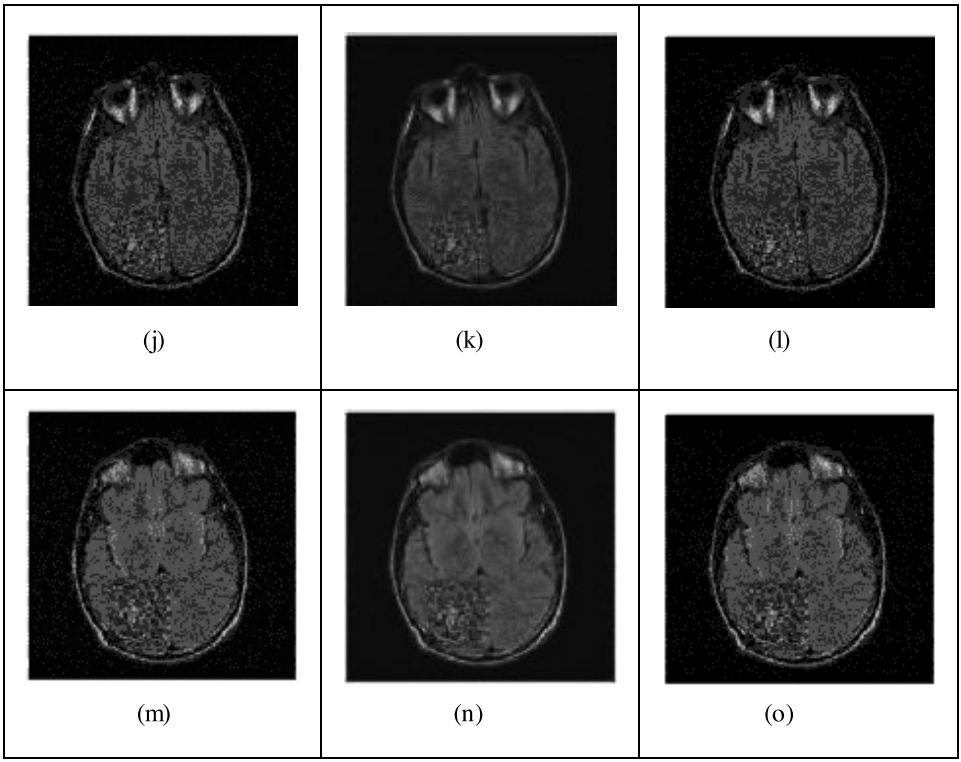

Fig. 5 (continued). Visual results of different sets of de-noised brain images using Curvelet Transform.

Segmentation of curvelet transform based de-noised image

The Image segmentation using fuzzy clustering algorithm has been applied to the following set of images.

Brain-3 Segmentation: This segmentation analysis is applied to the original image with no additional noise. As the image is transformed, it may have noise which affects the segmentation process.

Brain-3 Segmentation with white Gaussian noise at 40 dB: The higher noise level is selected to get better visual details.

Brain-3 Segmentation Curvelet-based de-noised image: Compared to noisy image, this segmentation analysis showed better results. Further investigations are required to improve the segmentation of de-noised image.

Class-4 is selected, because of its superior performance over other class. First selection of pattern detection is an image with prominent tumor. This image has strong possibility of correct diagnosis, even with the burst of noise covering the entire

malignant area. Figure 6(a) represents an original MR image with a relatively large size of malignant area. This contour of malignant pattern is under investigation for de-noising and segmentation. Figure 6(b) & Figure 6(c) are two segmentations of brain-3. Figure 6(b) defines the textures and the boundaries of the brain tissues. Similar results were obtained using repeated execution of the same code.

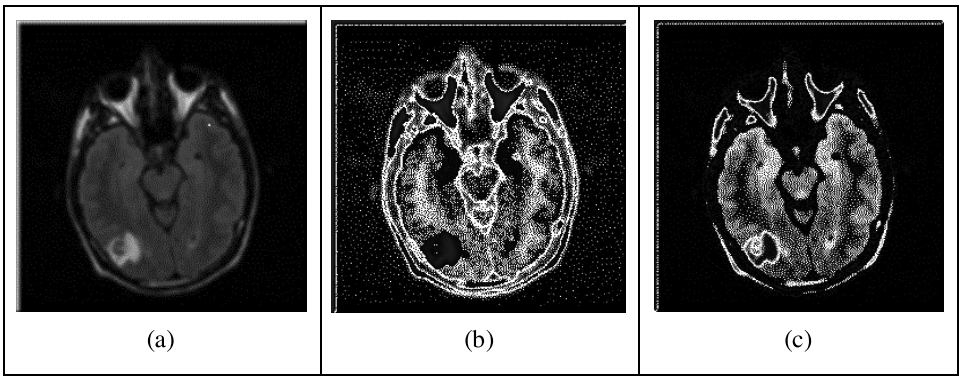

Fig. 6. Brain-3 Segmentation

Second selection of pattern detection is a noisy image with prominent tumor. This image showed poor segmentation, Figure 7 (a) shows a noisy MR image with relatively large size of malignant area. Figure 7 (b) & (c) are two segmentations of brain-3. This test has two major issues; first the image transformation adversely affected the quality of image and secondly the noise addition is also a source for sub-optimal segmentation.

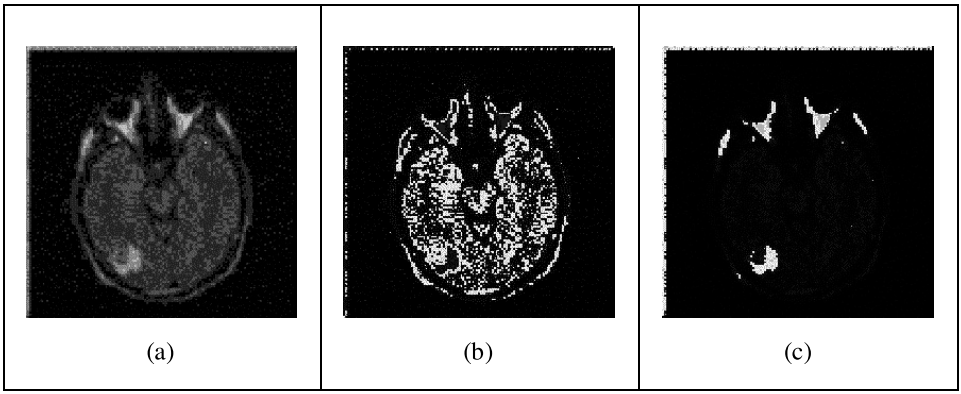

Fig. 7. Brain-3 Segmentation with white Gaussian noise of 40 dB

Third selection of pattern detection is a Curvelet based de-noised image with prominent tumor. This image showed poor segmentation. Figure 8 (a) shows de-noised MR image with large size of malignant area. Figure 8 (b) & (c) are two segmentations of brain-3. It is observed that image transformation is the major contributor for under-performance of the de-noising and segmentation. More studies are required to process image for suitable formats.

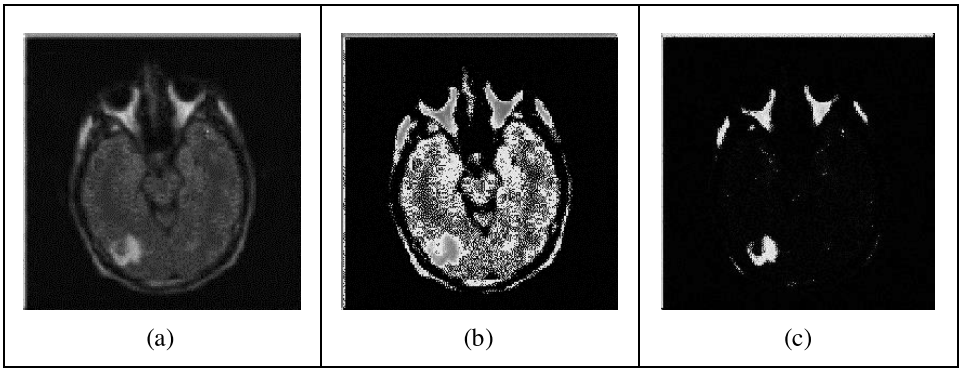

Fig. 8. Brain-3 Segmentation of Curvelet based de-noised image

Clustering of de-noised image is represented by FCM-class-4-dn; as shown in green colour in Figure 9 and in Table 5. The numbers of iterations are shown on the x-axis and cluster formations are shown on the y-axis. In the beginning cluster formations have a large number of cluster centers; that is about 2092 cluster centers. This process is settled at 669 cluster centers. Clustering of noisy image represents by FCM-class-4-noisy; as shown in red colour in Figure 9. Clustering of noisy image is represented by FCM-class-4-noisy; as shown in blue colour. This exercise also demonstrates the computations analysis of Curvelet Transform for segmented images.

Table 5. Class-4 clustering applied to image (De-noised Brain-3 using Curvelet Transform).

Iteration	FCM-class-4	FCM-class-4-noisy	FCFCM-class-4-dn
1	1896.509080	1966.397644	2092.878911
2	1452.244931	1499.518629	1595.036446
3	1450.793371	1497.970062	1594.600451
4	1432.535930	1476.196579	1590.448556
5	1269.732506	1240.747295	1559.461526
6	872.959855	639.180816	1425.289439
7	701.967399	551.077965	1146.244318
8	548.797846	384.581751	937.863385
9	468.245000	312.67428	742.662289
10	455.458868	299.072385	704.964964
11	433.924040	274.801369	683.151250
12	422.696302	212.706637	671.231428
13	421.679900	188.918456	669.430203

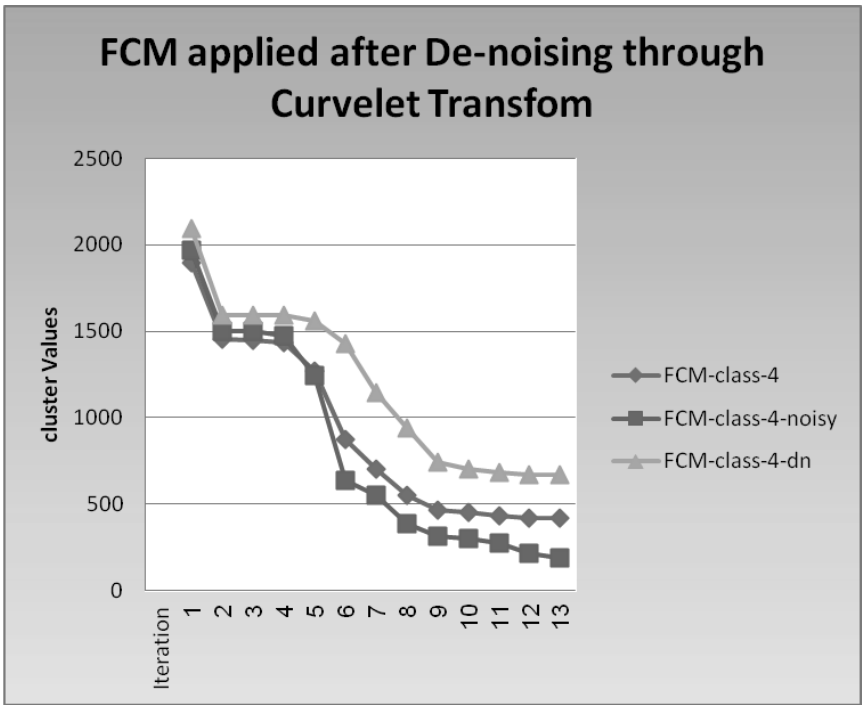

Fig. 9. Class-4 clustering applied to image (De-noised Brain-3 using Curvelet Transform).

CONCLUSION

Quality assessments are vital for many applications, such as acquisition, enhancement and reconstruction. This research has expounded on how non-homogenous noise influences the Curvelet Transform based image reconstruction. The scheme implemented here makes use of the Fuzzy C-Mean clustering algorithm for image segmentations. As the complexity of the images is unknown, combination of newer transforms could be used to de-noise different patterns of the image. The impact of non-homogeneous noise is not yet fully elucidated for image processing. In the future, fuzzy rule based thresholding will further improve for Ridgelets and Curvelets. From image segmentation analysis, it is concluded that the non-homogeneous noise distribution introduced significant difficulty to reconstruct the image. As a corollary of research, the problem of image segmentation has been addressed; thus making implementation complete.

In Summary:

1. In this research, we have presented image reconstruction aspects of first generation Curvelet Transform using Ridgelet Transform. The focus of the reconstruction included preserving edges and contours of the objects under investigation.

2. A brief comparative study has been performed on directional Wavelets such as Ridgelet, Contourlet and Curvelet as shown in Table 1 and Table 2.

3. The performance of the Curvelet Transform has been tested under clean, noisy and de-noised image as shown in Figure 1 and Figure 2.

4. The performance evaluations further under gone through non-homogeneous noise as shown in Figure 5. De-noising such images is an open challenge to Curvelet Transform.

5. Performance assessment of Curvelet Transform quantified through Peak Signal to Noise Ratio and Mean Square Error. Higher values support better performance claims of Curvelet Transform as shown in Figure 3 and Figure 4.

6. Perceptual assessments have been performed as shown in Figure 1 and Figure 2. In the reconstructed images, the curves and edges are preserved. These results demonstrate the superior performance of Curvelet Transform.

7. Segmentation of Curvelet Transform based de-noised images has been tested using Fuzzy C-Mean clustering algorithm as shown in Figure 6 to Figure 9. Segmenting image under noisy condition adversely affects the reconstruction performance of Curvelet Transform.

ACKNOWLEDGMENTS

We would like to thank Gilbert Strang, Mallat S.G., Rafael Gonzalez, and David Donoho for providing a theoretical frame work in image processing. Many thanks to Sandeep Palakkal from IIT Madras for providing Matlab based implementation of Curvelet and Ridgelet. We also wish to thank M. Misiti, Y. Misiti from The MathWorks, Inc for facilitating Matlab based implementation of Wavelet and to the Graduate School of Engineering Sciences and Information Technology, Hamdard University for their logistic support and services.

Portions of this work were presented and published in thesis form in fulfillment of the requirements for the PhD for RASHID HUSSAIN from *Hamdard University.*

REFERENCES

Bezdek, J. C. 1981. Pattern Recognition with Fuzzy Objective Function Algorithms. Kluwer Academic Publishers Norwell, MA, USA.

Bo Zhang. Fadili, J.M. & Starck, J.L. 2008. Wavelets, Ridgelets, and Curvelets for Poisson Noise Removal. IEEE Transactions on Image Processing **17**(7): 1093-1108.

Cannon, R. L. Dave, J. V. & Bezdek, J. C. 1986. Efficient implementation of the Fuzzy C-Means Clustering Algorithms. IEEE Transaction on Pattern Analysis and Machine Intelligence **8**(2): 248-255.

Candès, E. J. & Donoho, D.L. 1999. Curvelets : A Surprisingly Effective Non-adaptive Representation

for Objects with Edges; Curve and Surface Fitting: Saint-Malo Vanderbilt University Press, Nashville, USA.

Chen, G.Y., & Kégl B. 2007. Image de-noising with complex ridgelets, Pattern Recognition, **40**(2) 578 – 585.

Do M. & Vetterli, M. 2005. The Contourlet Transform: An efficient directional multi-resolution image representation. IEEE Transaction on Image Processing **14**(12):2091-2106.

Dunn, J.C. 1973. A fuzzy relative of the ISODATA process and its use in detecting compact well-separated clusters. Journal of Cybernetics **3**(3):32-57.

Esmaeili, M. Rabbani, H. Dehnavi, A.M. & Dehghani, A. 2012. Automatic detection of exudates and optic disk in retinal images using Curvelet Transform. IET Image Processing **6**(7): 1005-1013.

Feng, N. Liyong, Ma. & Shen, Ye. 2007. Fuzzy Partition Based Curvelets and Wavelets Denoise Algorithm, Computational Intelligence and Security Workshops.

Gonzalez R. & Wood R. 2002. Digital Image Processing, Pearson Education, Inc., 2nd edition.

Hussain, R. Sheeraz, A. Sikander, M. A. & Memon, A.R. 2011. Fuzzy clustering based malign areas detection in noisy breast Magnetic Resonant (MR) images. International Journal of Academic Research **3**(2) 65-70.

Kafieh, R. Rabbani, Hajizadeh, H. F. & Ommani, M. 2013. An Accurate Multimodal 3-D Vessel Segmentation Method Based on Brightness Variations on OCT Layers and Curvelet Domain Fundus Image Analysis. IEEE Transactions on Biomedical Engineering **10**(10): 2815- 2823.

Li, Q. W. Huo, G. Y. Li, H. Ma, G.C. & Shi, A. Y. 2012. Special section on biologically-inspired radar sonar systems - Bionic vision-based synthetic aperture radar image edge detection method in non-sub sampled contourlet transform domain Radar. IET Sonar & Navigation **6**(6): 526-53.

Lyer, N.S. Kandel, A. & Schneider, M. 2002. Feature-based fuzzy classification for interpretation of mammograms. Fuzzy Sets and Systems **114**(2):271–80.

Miri, M.S. & Mahloojifar, A. 2011. Retinal Image Analysis Using Curvelet Transform and Multistructure Elements Morphology by Reconstruction. IEEE Transaction on Biomedical Engineering **58**(5):1183-1192.

Starck, L. J. Candès, E.J. & Donoho, D.L. 2002. The Curvelet Transform for Image De-noising. IEEE Transaction on Image Processing **50**(3): 670-684.

Shen, Ji. Qin Li. & Erlebacher, G. 2011. Hybrid No-Reference Natural Image Quality Assessment of Noisy, Blurry, JPEG2000, and JPEG Images. IEEE Transactions on Image Processing **20**(8): 2089-2098.

Sheng-Hua Zhong. Yan Liu. Yang Liu & Chang-Sheng Li. 2013. Water Reflection Recognition Based on Motion Blur Invariant Moments in Curvelet Space. IEEE Transactions on Image Processing **22**(11): 4301- 4313.

Wen Liang, **H. Yeng M. S. & Chen, D. H. 2006.** Parameter selection for suppressed FCM with application to MRI. Pattern Recognition Letters **27**(5): 424-438.

Xinbo Gao. Wen Lu. Dacheng Tao & Xuelong Li. 2009. Image Quality Assessment Based on Multiscale Geometric Analysis. IEEE Transactions on Image Processing **50**(6):1409- 1423.

Submitted: 20-02-2014
Revised: 20-02-2014
Accepted: 20-10-2014